International Journal of HydroClimatic Engineering
Volume 1 Issue 1

Comparative Mapping of Flood-Susceptible Zones Using AHP and Machine Learning Models in a Data Scarce River Basin of Northeast India

Ashesh Rudra Paul[1] & Tilottama Chakraborty[2]

[1]Department of Civil Engineering, Indian Institute of Technology
Kharagpur, Kharagpur-721302, West Bengal, India

[2]Department of Civil Engineering, National Institute of Technology
Agartala, Jirania – 799046, West Tripura, India

Abstract

Flood-susceptible zone mapping is essential for effective flood risk management, enabling the identification of vulnerable areas and guiding targeted mitigation strategies. However, delineating flood-susceptible zones in data-scarce and topographically complex regions poses significant challenges. This study addresses these limitations by integrating Geographic Information Systems (GIS) with the Analytic Hierarchy Process (AHP) to assess flood susceptibility in the Haora River Basin, located in West Tripura, India. A total of nine flood-influencing parameters, including rainfall, elevation, slope, land use, and hydrological indices, were considered to develop a Flood Susceptibility Index (FSI). The resulting flood susceptibility map categorizes the basin into five classes: very low, low, moderate, high, and very high. The "Very High" zone covers 28.36 km², primarily concentrated in the low-lying urban areas around Agartala. The AHP model's predictive accuracy was validated using Receiver Operating Characteristic (ROC) curve analysis, which yielded an AUC of 0.848, indicating acceptable reliability. To enhance the robustness of the flood assessment, two machine learning models—Random Forest (RF) and Support Vector Machine

[1] Corresponding author, Email- asheshrudrapaul@gmail.com , ORCID: 0009-0007-2748-9183

(SVM)—were also employed. These models achieved AUC values of 0.9483 (RF) and 0.9260 (SVM), and demonstrated superior performance through lower MAE, MSE, and RMSE values compared to AHP. The integration of AHP-GIS with machine learning approaches offers a reliable and scalable framework for flood susceptibility mapping, especially in resource-limited environments. The methodology is generalizable to other vulnerable catchments across Northeast India and provides actionable insights for disaster planners and urban managers to prioritize high-risk zones and improve flood resilience.

Keywords: Flood-susceptibility mapping; Geographic Information Systems (GIS), Random Forest (RF), Support Vector Regression (SVM); Haora River Basin.

1. Introduction

Floods are among the most frequent and destructive natural hazards, inflicting severe impacts on human life, infrastructure, and ecosystems across the globe (Chaudhary & Piracha, 2021; Feng et al., 2023; Liu et al., 2023; Yu et al., 2022). These events not only damage property and agricultural areas but also disrupt transportation networks, displace populations, and result in long-term socio-economic setbacks, particularly in densely inhabited or agriculturally dependent regions (Alabbad et al., 2021; Hossain et al., 2024; Kumar et al., 2020). The intensity and frequency of floods are influenced by both natural factors—such as topography, climate variability, and hydrology—and human-induced activities, including unplanned urban expansion and deforestation (Hoang & Liou, 2024; Janizadeh et al., 2021; Pizzorni et al., 2024).

Flood-Susceptible Zones (FSZs) are areas with a heightened likelihood of inundation due to a combination of geomorphological and climatic factors (Jain & Singh, 2023; Kumar et al., 2023). Identifying these zones is a vital step toward effective flood risk mitigation, as it assists planners,

disaster managers, and decision-makers in formulating early warning systems, zoning policies, and protective infrastructure (Munpa et al., 2024; M. M. Rahman et al., 2024; Rana et al., 2021). The delineation of FSZs also enables a better understanding of flood dynamics, allowing for more informed planning and response strategies (Jha & Afreen, 2020; Samansiri et al., 2022; Agrawal et al., 2024; Munawar et al., 2021).

Traditionally, flood mapping relies on hydrological and hydraulic modeling or historical flood records. While these methods are valuable, they may not fully reflect future risks arising from climate change or rapid land use changes. As a result, there is increasing emphasis on advanced approaches that integrate multiple parameters. Among these, multi-criteria decision-making (MCDM) techniques, particularly the Analytic Hierarchy Process (AHP), have gained prominence. AHP enables both qualitative and quantitative criteria to be evaluated systematically by assigning relative weights based on expert judgment (Alam et al., 2024; Deo et al., 2024; Hadian et al., 2022).

The main strength of AHP lies in its structured approach to decomposing complex decision problems into a hierarchy, making it easier to compare the relative importance of contributing factors such as rainfall, slope, and land use (Hamizahrul, 2024; R. Kumar, 2025; H. U. Rahman et al., 2021; Rane et al., 2023). When used in conjunction with Geographic Information Systems (GIS), AHP becomes a powerful tool for spatial flood risk assessment, allowing for the visualization and analysis of flood susceptibility zones in a comprehensive manner (Efraimidou & Spiliotis, 2024; Leta & Adugna, 2023; Mabrouk & Haoying, 2023).

Despite these advances, the motivation behind this study stems from the pressing need to apply flood susceptibility models in data-scarce, high-risk basins like the Haora River Basin in Tripura, which remain largely underrepresented in current flood mapping literature. Rapid urbanization,

inadequate drainage infrastructure, and increasing rainfall variability in the region have made flood risk management more urgent than ever. Moreover, there is a growing demand to move beyond traditional AHP models and explore how machine learning-based approaches can complement or improve flood prediction accuracy, especially in regions where field data are limited or outdated.

Even though the widespread adoption of AHP-based flood mapping techniques, notable gaps remain in their application, particularly in under-studied, data-scarce regions. Most existing research focuses on well-instrumented river basins, leaving smaller and vulnerable catchments relatively unexplored. One such region is the Haora River Basin in West Tripura, India. Due to its monsoon-dominated climate, steep slopes, and rapid urban growth, this area is prone to recurrent flooding (Ahmed et al., 2024; Nath et al., 2024). However, limited efforts have been made to apply modern geospatial and decision-support methods for flood-prone zoning in this basin.

This study seeks to address that gap by applying a GIS-integrated AHP framework combined with machine learning (ML) models, such as Random Forest (RF) and Support Vector Machine (SVM), to assess flood risk in the Haora River Basin. This region is of strategic importance as it encompasses the state capital, Agartala, which frequently suffers from monsoonal floods due to inadequate drainage and urban encroachment (Debnath et al., 2022; Saha et al., 2021). Given the rising flood risk associated with climate extremes and land use change, developing a reliable flood-prone map for the Haora Basin is essential for sustainable urban planning and disaster risk reduction (Kumar, 2017; Saha et al., 2021).

A key novelty of this study lies in its integration of traditional AHP with advanced ML-based susceptibility modeling, thereby enabling a comparative evaluation between knowledge-driven and data-driven approaches. This dual-model framework enhances model robustness and allows validation of expert-based judgments through statistical accuracy metrics. Another major

contribution is the application of multicollinearity analysis (VIF and TOL) to ensure that flood-conditioning parameters are statistically independent, which is often overlooked in standard AHP-GIS studies. The study also addresses data integration challenges by resampling and harmonizing datasets with different spatial resolutions (e.g., Sentinel-2 LULC at 10 m and SRTM-derived layers at 30 m), ensuring spatial consistency in the modeling process.

By integrating key flood-influencing variables such as rainfall, elevation, slope, land use, and hydrological indices, this study develops a Flood Susceptibility Index (FSI). The performance of each model (AHP, RF, and SVM) is evaluated using the Receiver Operating Characteristic (ROC) curve analysis and the corresponding Area Under the Curve (AUC) values, as well as error metrics (MAE, MSE, RMSE) for ML models.

Therefore the final objective of this study is to develop a scientifically robust and spatially detailed flood susceptibility mapping framework for the Haora River Basin using a hybrid approach that integrates AHP and machine learning models (RF and SVM) within a GIS environment, with the aim of enhancing flood risk prediction in data-scarce, topographically complex regions like Tripura, and supporting evidence-based urban planning and disaster mitigation strategies.

2. Study Area

The Haora River is a significant watercourse located in the West Tripura District of the northeastern Indian state of Tripura. Geographically, the basin spans between 23°37′N to 23°53′N and 91°15′E to 91°37′E, as depicted in *Figure 1*. Covering a catchment area of approximately 405.8 square kilometers, the river system extends across both India and Bangladesh, with the majority of its expanse lying within southern West Tripura (Kumar, 2017). The basin is bordered

by the Khowai and Sepahijala Districts on the east and south, respectively, and by the international boundary with Bangladesh to the north and northwest.

The Haora River originates from the western slopes of the Baramura hill range. For the first 6.6 kilometers, the River flows through elevated, hilly terrain before descending into the foothill zone near Chandrasadhubari, situated at an altitude of 83 meters. From there, the River continues its course for about 21.8 kilometers through the middle catchment until it reaches the town of Jirania, where the elevation reduces to 32 meters. As it enters the plains, the River flows at altitudes below 30 meters until it eventually joins the Titas River in Bangladesh at a final elevation of 10 meters.

The overall length of the River is around 61.2 kilometers, with approximately 52 kilometers flowing through Indian territory (Bandyopadhyay et al., 2014). The region is characterized by gently undulating denudational terrain, locally known as "tilla lands," which vary in elevation from 6 to 201 meters. These tilla lands form part of the Dupitila geological formation and are primarily composed of sandy clay, clayey sandstone, and lateritic soils. These geological features significantly influence the basin's hydrological behavior, particularly its susceptibility to flood hazards.

The river basin's diverse topographical and geological setting renders it highly vulnerable to flood events, especially during periods of intense rainfall. Given the River's importance in sustaining water supply, agriculture, and infrastructure in the region, the Haora River Basin is a critical area requiring focused flood risk assessment. The variability in slope and landform across the basin adds to the complexity of flood response, making it imperative to adopt detailed spatial analysis for effective flood-prone area mapping and management.

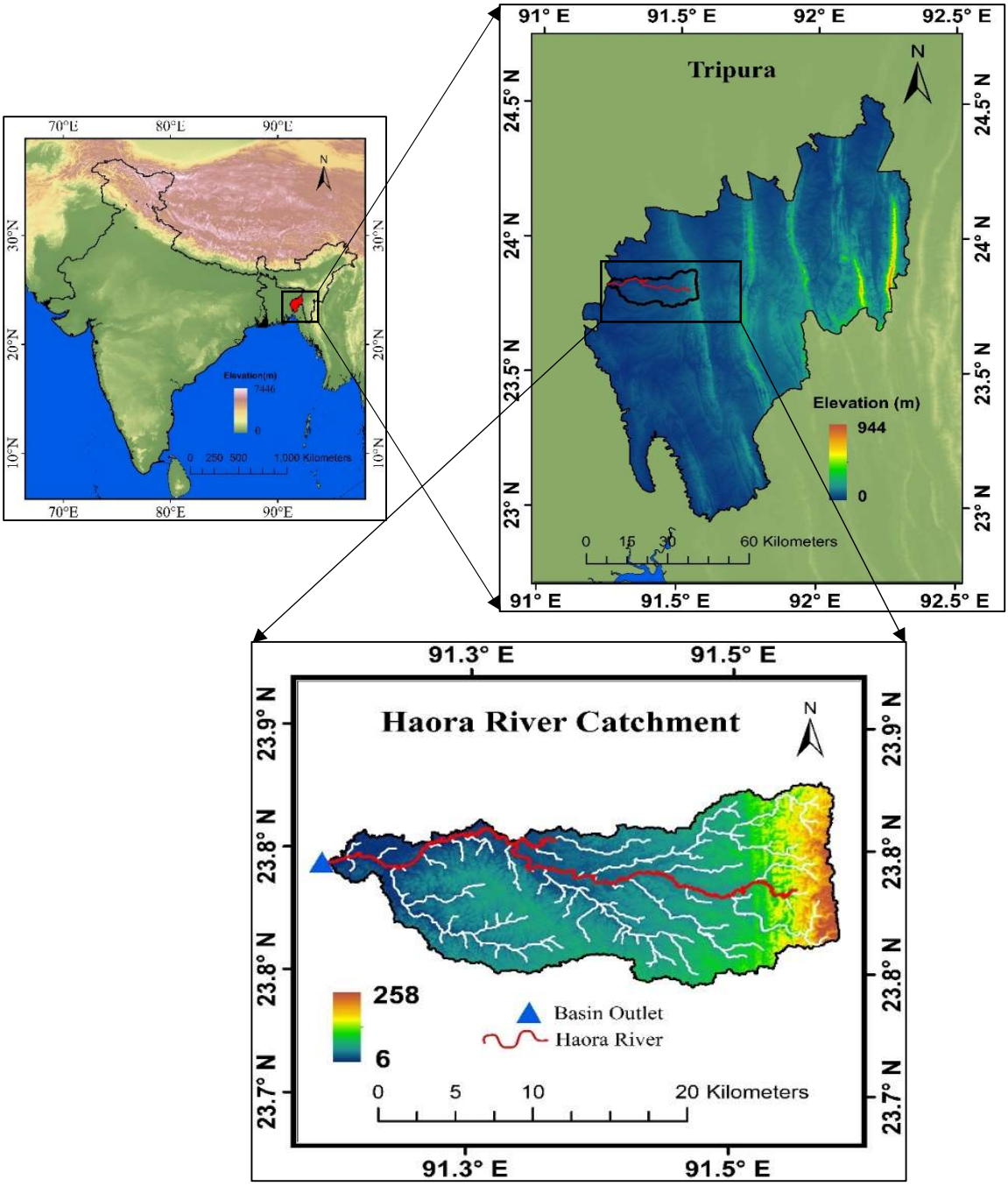

Figure 1: Geographical location of the Haora River Basin, highlighting the Study Area

3. Materials and Methods

This study adopts a multi-step framework to assess flood susceptibility in the Haora River Basin, employing both expert-based (AHP-GIS) and data-driven (machine learning) approaches. A total

of nine flood-conditioning parameters were selected based on hydrological, topographical, and geomorphological relevance: Rainfall, Elevation, Slope, Flow Accumulation, Proximity to River, Land Use and Land Cover (LULC), Topographic Wetness Index (TWI), Geomorphology, and Profile Curvature. The overall methodology consists of the following key steps:

Step 1: Multicollinearity Analysis

To ensure the independence of input variables, multicollinearity was assessed using Tolerance (TOL) and Variance Inflation Factor (VIF). Parameters with acceptable VIF values were retained for further analysis.

Step 2: Weight Assignment via AHP

The Analytic Hierarchy Process (AHP) was applied to derive the relative weights of the selected parameters based on expert judgment through a pairwise comparison matrix.

Step 3: FSI Map Generation via AHP-GIS

The weighted parameters were integrated using a GIS-based weighted overlay technique to generate a Flood Susceptibility Index (FSI) map, classified into five susceptibility zones.

Step 4: Machine Learning-Based Flood Susceptibility Modeling

To complement and compare with the AHP results, two machine learning algorithms, such as RF and SVM, were applied using the same set of input variables.

Step 5: Sensitivity Analysis of AHP Weights

To evaluate the robustness of AHP-derived weights, a sensitivity analysis was performed using the Stillwell ranking method, incorporating Rank Sum Weight (RSW) and the Reciprocal Rank Weight (RRW) techniques.

Step 6: Model Validation

All three models (AHP, RF, and SVM) were validated using Area Under the Receiver-Operating Characteristic Curve (AUC-ROC) analysis, while RF and SVM were further evaluated using Mean Absolute Error (MAE), Mean Square Error (MSE), and Root Mean Square Error (RMSE) to assess predictive performance.

An overview of the entire methodological workflow is presented in Figure 2.

3.1.Data Collection and Processing

The data for this study were sourced from various reliable and authoritative databases to ensure comprehensive analysis and accurate flood-prone region mapping in the Haora River Basin. The primary parameter used is rainfall, with data spanning from 1981 to 2023, obtained from the India Meteorological Department (IMD).

This dataset is crucial for understanding the temporal and spatial variations in precipitation, which significantly influence flood events in the region. LULC data were obtained using Sentinel-2 satellite imagery at a 10m resolution for the year 2022—the LULC map, accessible through the Living Atlas platform (https://livingatlas.arcgis.com/landcoverexplorer/#mapCenter=-3.28600%2C31.34000%2C3&mode=step&year=2022, accessed in Jan 2025). For elevation data, a Digital Elevation Model (DEM) with 30m resolution was used, sourced from the USGS Earth Explorer (https://earthexplorer.usgs.gov/, accessed in Jan 2025). This DEM is pivotal for calculating the slope and other terrain-related parameters, which influence water flow and flood behavior in the basin. Geological and geomorphological data were sourced from the Geological Survey of India's Bhukosh database (https://bhukosh.gsi.gov.in/Bhukosh/Public, accessed in Jan

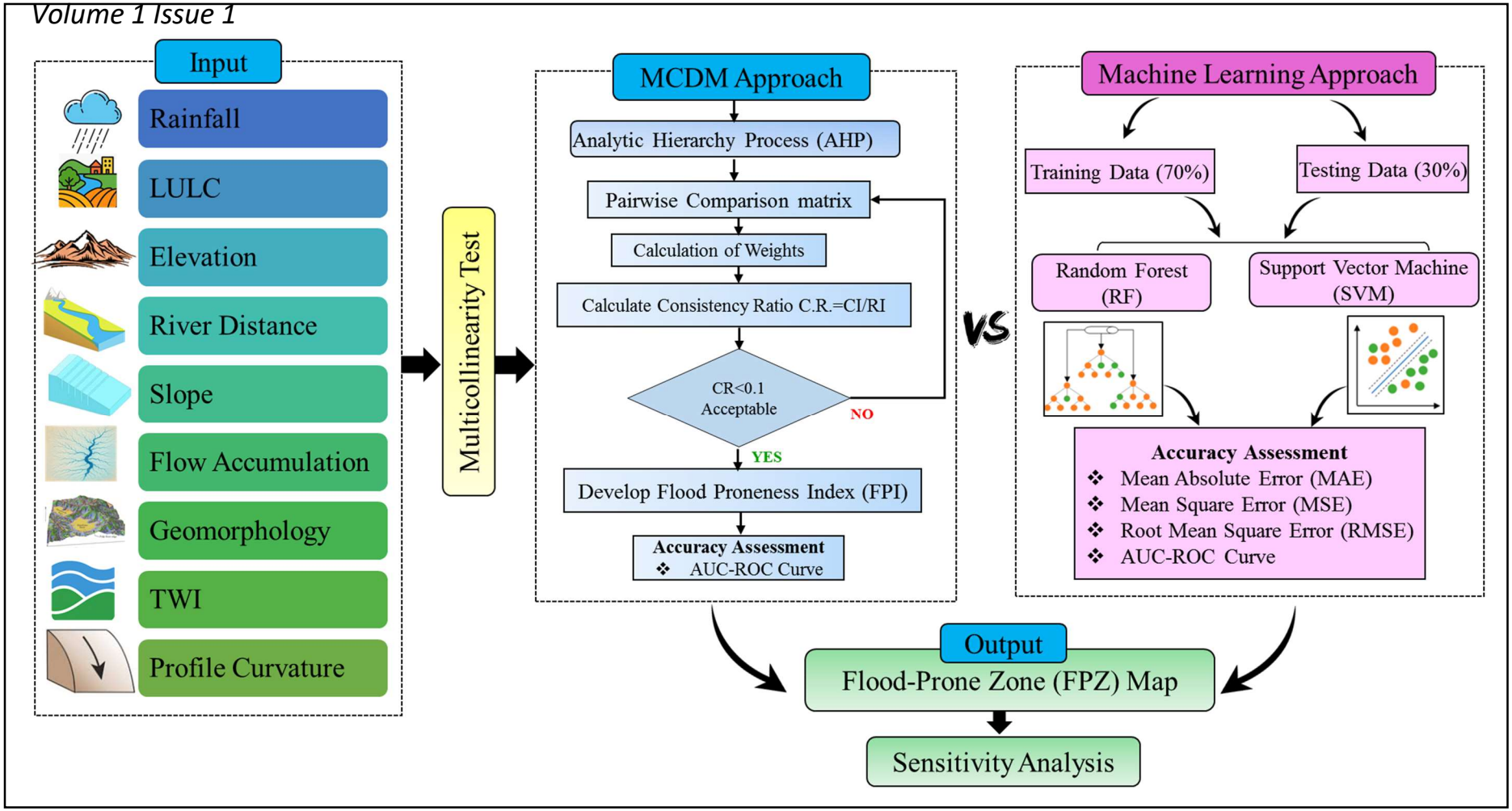

Figure 2: Methodological flowchart for flood susceptibility mapping in the Haora River Basin using Analytic Hierarchy Process (AHP), Random Forest (RF), and Support Vector Machine (SVM) Method

183 2025), providing insights into the regional geological structure and terrain, which directly affect
184 flood dynamics and the River's morphological changes.

185 To address the spatial resolution mismatch between Sentinel-2 (10 m) and DEM (30 m), all input
186 layers were resampled to a uniform 30 m grid using bilinear interpolation for continuous data and
187 nearest-neighbor interpolation for categorical data (e.g., LULC). This harmonization ensured
188 spatial consistency in model inputs and avoided distortion in classification outputs during GIS-
189 based overlay and machine learning analysis.

190 Table 1: Parameters, descriptions, and data sources used for identifying flood-prone areas

Parameters	Description	Sources
Rainfall (mm)	Rainfall data for the period 1981–2023.	India Meteorological Department (IMD) (https://www.imdpune.gov.in/cmpg/Griddata/Rainfall_25_NetCDF.html)
LULC	Land Use Land Cover map was obtained using Sentinel-2 satellite data.	Sentinel-2 10m Land Use/Land Cover (https://livingatlas.arcgis.com/landcoverexplorer/#mapCenter=-3.28600%2C31.34000%2C3&mode=step&year=2022)
Elevation (m)	Elevation data with 30 m resolution.	USGS Earth Explorer (https://earthexplorer.usgs.gov/)
Geomorphology	Geological and geomorphological data.	GSI Bhukosh (https://bhukosh.gsi.gov.in/Bhukosh/Public)
Proximity to the River (km)	Calculated as the distance from the nearest River using a river shape file in ArcGIS.	Derived using ArcGIS tools and a river shape file.
Slope (Degree)	Slope calculated using the Digital Elevation Model (DEM).	Derived using ArcGIS tools and DEM.
Flow Accumulation (pixels)	Flow accumulation values are determined from the DEM.	
Topographic Wetness Index (TWI)	Indicator of topographic control on hydrological processes, derived from DEM data.	
Profile Curvature	Describes the curvature of the terrain surface, calculated from DEM.	

191 The distance from the River to key locations in the study area was calculated using a river shapefile
192 and ArcGIS tools. This parameter is important for understanding the proximity of flood-prone

areas to the River, which influences flood risk. Slope data, calculated from the DEM, were derived using ArcGIS tools. The slope of the terrain plays a critical role in determining surface runoff, which in turn impacts the extent and severity of flooding. Flow accumulation values, derived from the DEM, help in identifying areas that contribute to runoff and are susceptible to flooding. This was complemented by the calculation of the TWI, which indicates the topographic control on hydrological processes, derived from the DEM data. Finally, profile curvature, which describes the curvature of the terrain surface, was calculated from the DEM and is helpful in understanding water flow patterns and potential flood hotspots. All these data parameters were integrated into GIS software for spatial analysis and flood susceptibility mapping in the Haora River Basin.

To address the challenge of limited ground-based data, the study used freely available remote sensing datasets and hydrological indices derived from DEMs and satellite imagery. Parameters were selected based on their relevance and accessibility in similar data-scarce environments. Additionally, AHP was employed for expert-based weighting where empirical data was limited, and ML models were trained using minimal but verified historical flood occurrence points. The description of all these data parameters is summarized in tabulated form in *Table 1*.

3.2.Preparation of thematic layers

As part of the present study, nine thematic layers were selected as flood susceptibility parameters for the Haora River Basin. The methodology for selecting and processing the flood susceptibility parameters is explained in detail below. The thematic layers of all parameters are visualized in *Figure 3* to provide a clear spatial representation of the data utilized in this study.

The selection of these nine flood-conditioning parameters was based on their demonstrated relevance to flood generation and propagation, as supported by hydrological theory and previous

flood susceptibility studies (Kaya & Derin, 2023; Swain et al., 2020; Tehrany et al., 2014). Core parameters like rainfall, elevation, slope, and flow accumulation control runoff and accumulation dynamics, while LULC, TWI, and proximity to rivers influence infiltration and flood exposure. Geomorphology and profile curvature provide terrain-specific insights into water flow and accumulation patterns. Together, these layers represent a comprehensive set of biophysical factors that drive flooding in the Haora River Basin.

3.2.1. Rainfall

Rainfall significantly influences river discharge and flood risk. The rainfall pattern in the Haora River Basin was interpolated using the Inverse Distance Weighting (IDW) method to create a rainfall map. Areas with higher rainfall were assigned higher ranks, indicating an increased likelihood of flooding. The rainfall distribution map is an essential component of the flood-prone area assessment.

3.2.2. LULC

LULC significantly impacts runoff patterns and groundwater quality, with built-up areas and barren lands promoting higher surface runoff and vegetated areas encouraging water infiltration. In the Haora River Basin, urban areas, which are more vulnerable to flooding, were assigned the highest rank (rank 5) due to their high contribution to flood risk.

3.2.3. Elevation

Elevation plays a crucial role in water flow, with water generally flowing from higher to lower elevations, accumulating in lower areas. A Jenks natural breaks method was used to classify Haora River Basin elevation data into five distinct classes. Lower elevation zones, which are more prone to water accumulation, were assigned higher ranks, indicating a higher contribution to flood vulnerability.

3.2.4. Geomorphology

Geomorphology significantly influences flood susceptibility in the Haora River Basin. The land is categorized into five geomorphological classes: Flat Areas (Rank 5), which are highly prone to flooding due to poor drainage; and Steep Areas (Rank 1), which experience rapid runoff and are less prone to flooding. These classifications help assess flood risk across different terrains of the basin.

3.2.5. Proximity to the River

Distance from the River is a crucial parameter in flood risk assessment, as areas located close to the River are at a higher risk of flooding. A buffer zone of 2 km intervals was created along both sides of the Haora River using ArcGIS. Higher flood risk was assigned to areas within a 2 km distance from the River, while areas further away (6–8 km) were given lower ranks, indicating reduced flood risk.

3.2.6. Slope

Slope is a significant factor influencing water accumulation, as areas with low or gentle slopes tend to retain more water. The Haora River Basin has relatively gentle slopes in the central floodplain area, which increases the risk of flooding. On the other hand, steeper slopes are found in the surrounding hilly regions. The slope was classified into different categories based on the gradient, with lower slopes assigned higher ranks for increased flood susceptibility.

3.2.7. Flow Accumulation

Flow accumulation represents the sum of water flowing down a slope into cells of the output raster. In the Haora River Basin, flow accumulation varies from 0 to 220553, with lower values observed near lower-order stream confluences and higher values near higher-order stream confluences. As

a result of high accumulation areas being more vulnerable to flooding, the parameter was divided into five classes using the Jenks natural breaks method. Flow accumulation identifies areas where surface runoff converges, which are typically more susceptible to inundation (Bales & Wagner, 2009; Prokešová et al., 2022). In regions like the Haora Basin, where rainfall intensity is high and drainage is constrained, this parameter helps pinpoint natural water collection zones

3.2.8. Topographic Wetness Index (TWI)

The TWI reflects the influence of topography on hydrological processes, especially runoff and accumulation of flows. It was calculated using the equation.

$$TWI = \ln(\alpha/\tan\beta) \quad (1)$$

where, α is the contributing area at the upslope and β is the topographic gradient. Higher TWI values indicate areas more vulnerable to flooding due to greater water accumulation. For the Haora River Basin, areas with higher TWI values were assigned higher ranks, contributing significantly to flood susceptibility.

3.2.9. Profile Curvature

Profile curvature indicates the direction of maximum slope. Concave surfaces (positive curvature values) accelerate flow and encourage water accumulation, while convex surfaces (negative curvature values) decelerate flow and reduce water accumulation. In this study, areas with positive curvature were assigned higher ranks for flood susceptibility, as they facilitate water accumulation. Profile curvature influences the acceleration or deceleration of flow, which in turn affects erosion and deposition processes. Positive (concave) curvature zones tend to accumulate water, making them locally relevant for flood-prone mapping (Idrees et al., 2022).

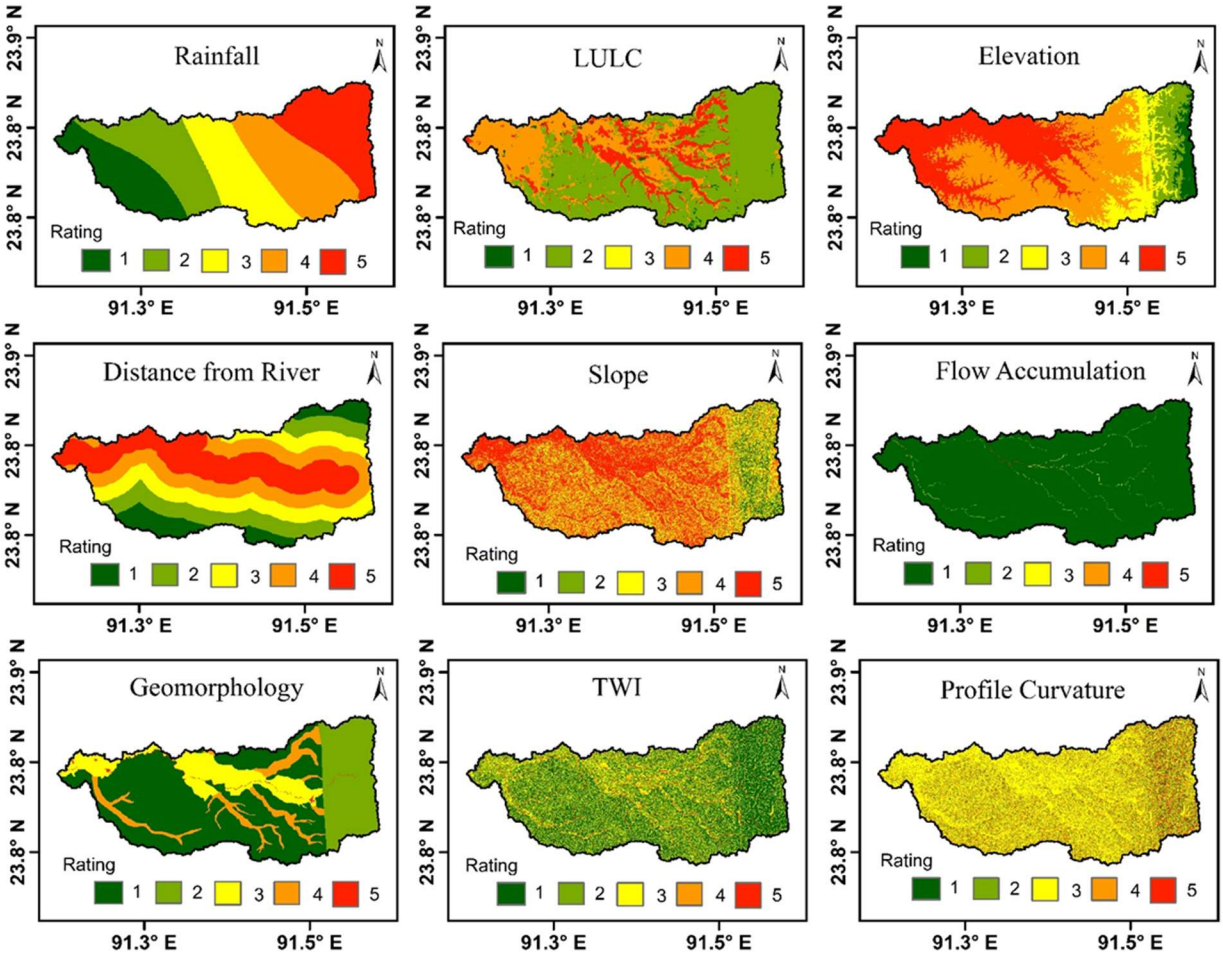

Figure 3: Reclassified Thematic Map of Input Parameters Used for AHP Method, Ranked from Very Low (1) to Very High (5)

To ensure the robustness of the flood susceptibility modeling, a multicollinearity analysis was conducted among the selected flood-influencing factors. Multicollinearity refers to a statistical phenomenon where two or more predictor variables in a model are highly correlated, potentially leading to unreliable estimates of their individual contributions. Its presence can inflate the variance of model coefficients and compromise the interpretability of both statistical and machine learning models. Therefore, prior to applying any modeling techniques, it was essential to examine the interrelationships among the independent variables.

3.3.Multicollinearity Analysis

To ensure the robustness and statistical validity of the flood susceptibility modeling, a multicollinearity analysis was conducted among the selected flood-influencing factors. Multicollinearity refers to a condition where two or more predictor variables are highly correlated, potentially inflating the variance of coefficient estimates and compromising the stability and interpretability of both statistical and machine learning models (Saha et al., 2023). Addressing multicollinearity is essential before applying regression-based or model-based techniques to avoid biased weight estimations and misinterpretation of variable importance (Mukherjee & Singh, 2020).

In this study, two standard diagnostic measures were employed to assess multicollinearity: Tolerance (TOL) and the Variance Inflation Factor (VIF). Tolerance measures the proportion of a variable's variance that is not explained by other predictors in the model, with values closer to zero indicating stronger multicollinearity. The VIF, which is the reciprocal of tolerance, indicates how much the variance of an estimated regression coefficient increases due to collinearity. The VIF, introduced by Marquardt (1970), is the reciprocal of tolerance and quantifies how much the variance of a regression coefficient is inflated due to multicollinearity. The mathematical expressions are as follows:

$$TOL_j = 1 - {R_j}^2 \tag{2}$$

$$VIF_j = \frac{1}{TOL_j} \tag{3}$$

Where, ${R_j}^2$ is the coefficient of determination when the j^{th} predictor is regressed against all other predictors. In general, a VIF value greater than 10 or a Tolerance value less than 0.1 is considered

313 indicative of serious multicollinearity that may require corrective measures, such as variable
314 elimination or transformation.

315 In this analysis, all selected variables were found to have acceptable TOL and VIF values,
316 indicating that they were sufficiently independent and could be retained for further modeling. This
317 diagnostic step ensured that the input variables used in the AHP-based MCDM and machine
318 learning models (RF and SVM) were statistically valid and free from redundancy, thereby
319 enhancing the reliability of the flood susceptibility assessment.

320 **3.4.Application of MCDM and Development of Flood Susceptibility Index (FSI)**

321 To evaluate flood risk across the Haora River Basin, this study employed an MCDM framework
322 to rank and weight key flood-influencing parameters. Specifically, the AHP was utilized to
323 determine the relative importance of the nine selected indicators. The AHP technique is well-
324 regarded for its structured approach in decision-making, especially when handling both qualitative
325 and quantitative inputs (Hadian et al., 2022; Paul, A.R., Saha, 2021). AHP was chosen over other
326 MCDM methods due to its suitability in data-scarce regions, its structured expert-driven design,
327 and its wide adoption in flood risk mapping under similar conditions.

328 Initially introduced by T.L. Saaty in the late 1970s, AHP facilitates the prioritization of factors by
329 structuring complex problems into a hierarchy, enabling systematic pairwise comparisons (Saaty,
330 1990, 2004). In the context of this study, AHP was used to compute weights for each thematic
331 parameter contributing to flood susceptibility in the Haora catchment. These weights were later
332 integrated to develop the Flood Susceptibility Index (FSI).

333 *Step 1: Pairwise Comparison Matrix (PCM)*

The first step involved constructing a pairwise comparison matrix (PCM), where each element represents the relative importance of one parameter compared to another. We compared the importance of the factors using Saaty's scale from 1 (equal importance) to 9 (extreme importance) (see *Table 2*).

Table 2: Saaty's Fundamental AHP Scale

Importance level	Description
1	Equal importance
3	Moderate importance
5	Strong importance
7	Very strong importance
9	Extreme importance
2,4,6,8	Intermediate values

For instance, if rainfall is considered far more critical than geomorphology, a higher score is assigned to the rainfall-to-geomorphology cell, and the reciprocal value is assigned to the inverse comparison. The general structure of the PCM is expressed as:

$$A = \begin{bmatrix} 1 & a_{12} & a_{13} & \dots & a_{19} \\ \frac{1}{a_{12}} & 1 & a_{23} & \dots & a_{29} \\ \frac{1}{a_{13}} & \frac{1}{a_{23}} & 1 & \dots & a_{39} \\ \vdots & \vdots & \vdots & \ddots & \vdots \\ \frac{1}{a_{19}} & \frac{1}{a_{29}} & \frac{1}{a_{39}} & \dots & 1 \end{bmatrix} \quad (4)$$

Step 2: Weight Calculation

Once the PCM is populated, the next step is to compute the relative weights of the factors. This is achieved by calculating the geometric mean of each row in the PCM. The geometric mean for the i^{th} factor is computed as:

$$GM = \sqrt[n]{a_{i1} \times a_{i2} \times \dots \times a_{i9}} \quad (5)$$

where $n = 9$ is the total number of factors, and a_{ij} represents the matrix elements. To normalize these weights, each geometric mean is divided by the sum of all geometric means:

$$w_i = \frac{GM_i}{\sum_{i=1}^{n} GM_i} \tag{6}$$

where w_i is the normalized weight for the i^{th} factor, reflecting its relative importance in influencing Flood Susceptibility within the Haora River catchment.

Step 3: Consistency Check

To ensure the reliability of the judgments used in the matrix, a consistency ratio (CR) was calculated. First, the maximum eigenvalue (λmax) of the matrix is estimated, followed by computing the consistency index (CI):

$$CI = \frac{\lambda_{max} - 1}{n - 1} \tag{7}$$

The consistency ratio is then derived using:

$$CR = \frac{CI}{RI} \tag{8}$$

where RI stands for Random Index, reliant on the matrix size. If CR≤0.10, the level of consistency is deemed acceptable.

Step 4: Calculation of Flood Susceptibility Index (FSI)

Once the ranks and weights were finalized, the Flood Susceptibility Index was computed using the weighted sum of ranked values for each parameter:

$$FSI = \sum_{i=1}^{n} w_i \times r_i \tag{9}$$

where, w_i is the weight of the i^{th} parameter and r_i is the rank assigned to that parameter for a particular spatial unit. The final FSI values were used to classify the study area into five flood risk categories—'Very Low', 'Low', 'Moderate', 'High', and 'Very High'. This classification facilitates targeted intervention and prioritization for flood mitigation. The FSI map highlights critical zones, aiding stakeholders in decision-making related to flood preparedness and land use planning.

To ensure comparability among input parameters with differing units and scales, all thematic layers were normalized using a rank-based reclassification approach. Each layer was divided into five ordinal classes, ranked from 1 (very low susceptibility) to 5 (very high susceptibility), based on hydrological logic and their relative influence on flood generation. For instance, areas with low elevation, high rainfall, gentle slopes, and proximity to the river were assigned higher ranks due to their greater flood potential. Continuous variables (e.g., elevation, slope, flow accumulation) were reclassified using the Jenks natural breaks method, while categorical variables (e.g., LULC, geomorphology) were ranked based on flood vulnerability from prior studies and expert judgment. This standardization allowed all layers to be integrated through the weighted overlay technique in GIS to generate the FSI map.

3.5. Machine Learning-Based Flood Susceptibility Modeling

To develop an accurate flood susceptibility map for the study area, two supervised machine learning algorithms—Random Forest (RF) and Support Vector Machine (SVM)—were applied. These algorithms were chosen due to their proven effectiveness in handling complex nonlinear relationships and high-dimensional environmental datasets. The modeling process utilized nine flood-conditioning factors, and the corresponding flood inventory data were randomly divided into 70% training and 30% testing subsets to ensure balanced representation of flooded and non-flooded classes.

3.5.1 Random Forest (RF)

Random Forest is an ensemble learning algorithm that builds multiple decision trees using different subsets of training data and predictor variables. Each decision tree makes an individual prediction, and the final classification is determined through a majority voting scheme. This method reduces overfitting and improves model robustness. In this study, the RF model was trained using the 70% training subset, while the remaining 30% was used for testing. The number of trees and the number of features considered at each split were optimized through grid search and cross-validation techniques. The underlying principle and flow of the Random Forest algorithm used in this study are visually depicted in *Figure 4,* which shows how multiple trees contribute to the final classification through majority voting.

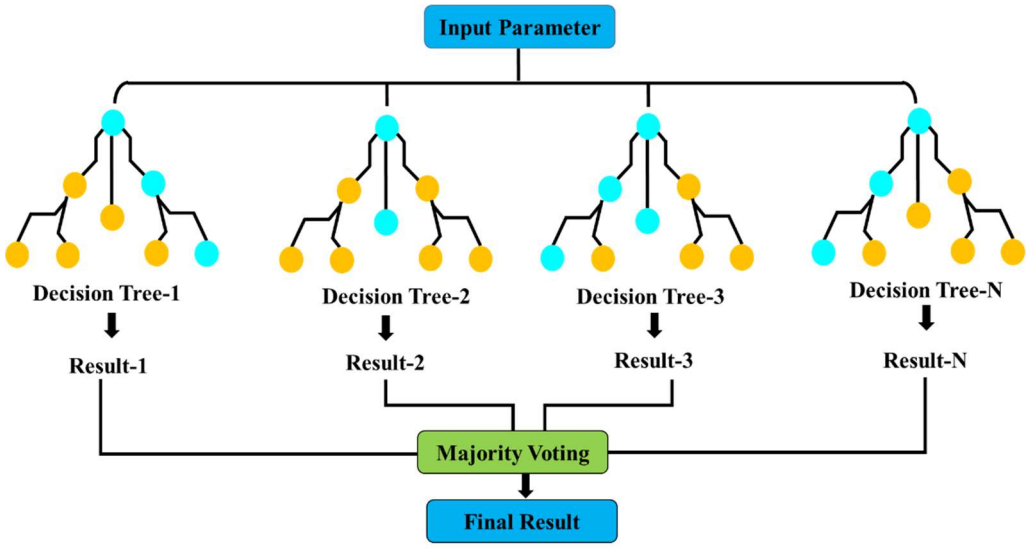

Figure 4: General schematic representation of the Random Forest (RF) algorithm, illustrating how multiple decision trees contribute to the final prediction through majority voting.

3.5.2 Support Vector Machine (SVM)

Support Vector Machine is a powerful classification technique that aims to identify an optimal boundary between different classes in the feature space. For datasets that are not linearly separable, SVM applies a kernel function to transform the data into a higher-dimensional space, where a clear

decision boundary can be established. In this study, the Radial Basis Function (RBF) kernel was used due to its effectiveness in environmental modeling tasks.

The model was trained on the 70% training data and tested on the 30% holdout set. Key parameters, including the penalty parameter and kernel coefficient, were fine-tuned using grid search with 10-fold cross-validation. The model's performance was assessed using the same evaluation metrics as RF to ensure consistency. A conceptual overview of the SVM model applied in this study is illustrated in *Figure 5*, highlighting the use of kernel transformations and the classification process.

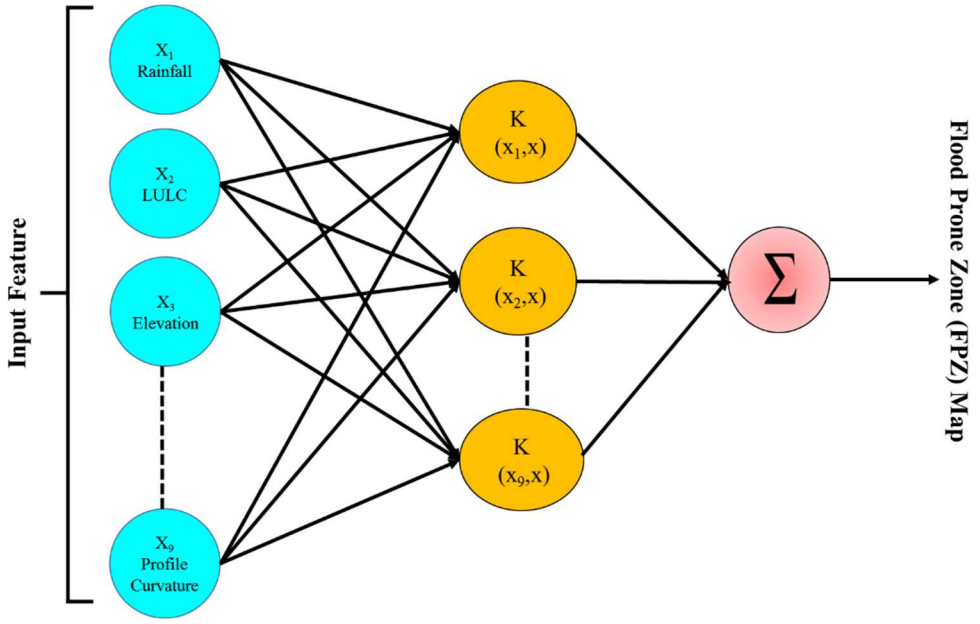

Figure 5: General schematic of the Support Vector Machine (SVM) model using a Radial Basis Function (RBF) kernel. Input features are transformed into a higher-dimensional space through kernel functions to identify the optimal hyperplane for classification.

Both RF and SVM models were implemented using the scikit-learn library in Python. The trained models were applied to spatial predictor layers within a GIS environment to produce flood susceptibility maps across the study region.

To assess the performance and generalization ability of the machine learning models during both training and validation, several statistical evaluation metrics were employed. These include Mean

Absolute Error (MAE), Mean Square Error (MSE), and Root Mean Square Error (RMSE). These metrics quantify the difference between predicted and observed class labels or values and provide insights into model accuracy and reliability. The equations used to compute these indices are as follows:

$$MAE = \frac{1}{n}\sum_{i=1}^{n}|y_i - \widehat{y_i}| \tag{10}$$

$$MSE = \frac{1}{n}\sum_{i=1}^{n}(y_i - \widehat{y_i})^2 \tag{11}$$

$$RMSE = \sqrt{MSE} \tag{12}$$

where, n is the total number of observations, y_i is the actual observed value, and $\widehat{y_i}$ is the predicted value from the model. These error metrics were computed for both the training and testing phases to support the classification metrics (accuracy, precision, etc.) and provide a comprehensive evaluation of model performance in flood susceptibility mapping.

3.6.Sensitivity-Based Validation of AHP Parameter Weighting

While the AHP is a powerful tool for assigning weights to criteria, it involves a degree of subjectivity, particularly in how weights are derived from expert judgment. To strengthen the credibility of the model, this study incorporated a sensitivity analysis using the Stillwell ranking technique. Through the comparison of the AHP-derived weights with alternative ranking methods, we provide cross-validation of the weights developed by AHP.

According to Stillwell's ranking method, two comparative weighting functions can be used: the Rank Sum Weight (RSW) and the Reciprocal Rank Weight (RRW). These methods are useful for

validating how different ranking strategies affect the distribution of weights assigned to each parameter. The two weighting approaches are defined as follows:

$$W_i^{RS} = \frac{(n - R_j + 1)}{\sum_{j=1}^{n}(n - R_j + 1)} \tag{13}$$

$$W_i^{RR} = \frac{\frac{1}{R_j}}{\sum_{j=1}^{n}\frac{1}{R_k}} \tag{14}$$

Here, W_i^{RS} and W_i^{RR} represent the normalized weights derived from the Rank Sum and Reciprocal Rank methods, respectively. In these equations, n is the total number of attributes being analyzed. R_j is the rank assigned to the j^{th} attribute, arranged in ascending order based on importance. W_i^{RS} normalizes the weights by dividing the rank-adjusted values by their total sum. W_i^{RR} normalizes weights based on the reciprocal of the ranks. This approach provides an additional layer of validation, enabling a comparative evaluation of the weights generated by AHP and ensuring consistency in the prioritization of factors influencing flood vulnerability.

3.7. Validation of Flood Susceptibility Zone (FSZ) Map Using ROC-AUC

In this research, the FSZ map for the Haora River Basin has been validated using the ROC-AUC method. This statistical approach is widely recognized for evaluating the performance of predictive models and provides an effective measure of the accuracy of spatial predictions. ROC-AUC analyses are particularly useful for assessing the accuracy of FSZ maps in identifying flood-prone areas. As a result, a model's sensitivity and specificity are assessed objectively, allowing an objective review of its performance (Darabi et al., 2020; Ghosh et al., 2022; Vilasan & Kapse, 2022). The observed flood data for the Haora River Basin, collected and reported by Chakraborty & Pan (2012) and Kuntal (2015), have been used as the ground truth for validation purposes.

In the two-dimensional ROC plot, the vertical axis denotes sensitivity (i.e., the true positive rate), while the horizontal axis represents 1 minus specificity, corresponding to the false positive rate. These parameters are mathematically defined using equations derived by Swets (1988):

$$x = 1 - Specificity = 1 - \frac{TN}{TN+} \quad (15)$$

$$y = Sensitivity = \frac{TP}{TN+FN} \quad (16)$$

Here, TP refers to true positive locations that are accurately classified as flood-prone areas, while TN indicates true negatives, which are correctly identified as regions not susceptible to flooding. FP represents false positives, where areas are mistakenly classified as flood-prone, and FN corresponds to false negatives, where flood-prone areas are incorrectly labeled as non-flood-prone. The ROC curve is plotted based on these parameters, and the area under the curve (AUC) quantifies the model's predictive performance. An AUC value closer to 1 indicates excellent predictive accuracy, while a value around 0.5 reflects a model with no discriminative power.

4. Results and Discussion

4.1. Multicollinearity Analysis

The results of the multicollinearity analysis for the nine selected flood-conditioning factors are presented in *Table 3*, based on the computed Tolerance (TOL) and Variance Inflation Factor (VIF) values.. All variables exhibited TOL values well above the critical threshold of 0.1 and VIF values below 10, indicating the absence of significant multicollinearity among the predictors. Specifically, TOL values ranged from 0.374 to 0.703, while the corresponding VIF values varied between 1.421 and 2.673. These findings suggest that the selected variables are sufficiently independent and do not exhibit problematic intercorrelation that could distort model estimation or interpretation.

Table 3: The computed TOL and VIF values for the nine selected variables

	TOL	VIF
Rainfall	0.477	2.096
Elevation	0.479	2.088
Slope	0.648	1.543
Proximity to the River	0.594	1.684
Flow Accumulation	0.512	1.951
TWI	0.374	2.674
LULC	0.464	2.154
Geomorphology	0.703	1.541
Profile Curvature	0.703	1.421

4.2. Results of AHP-Based Flood Susceptibility Mapping

This study focuses on identifying flood-prone zones in the Haora River Basin of the West Tripura district using the AHP within a GIS environment. A total of nine parameters that are strongly associated with flood susceptibility were integrated to develop the composite FSI. The final flood-prone zoning (FSZ) map was created by categorizing the FSI values into five distinct classes. These classifications were determined using the equal interval classification method, where FSI values ranged from 0 to 1. The resulting FSZ map for the Haora River Basin is presented in *Figure 6*, providing a visual representation of the flood susceptibility levels across the study area. This classification approach provided a systematic representation of the varying levels of flood susceptibility across the study area.

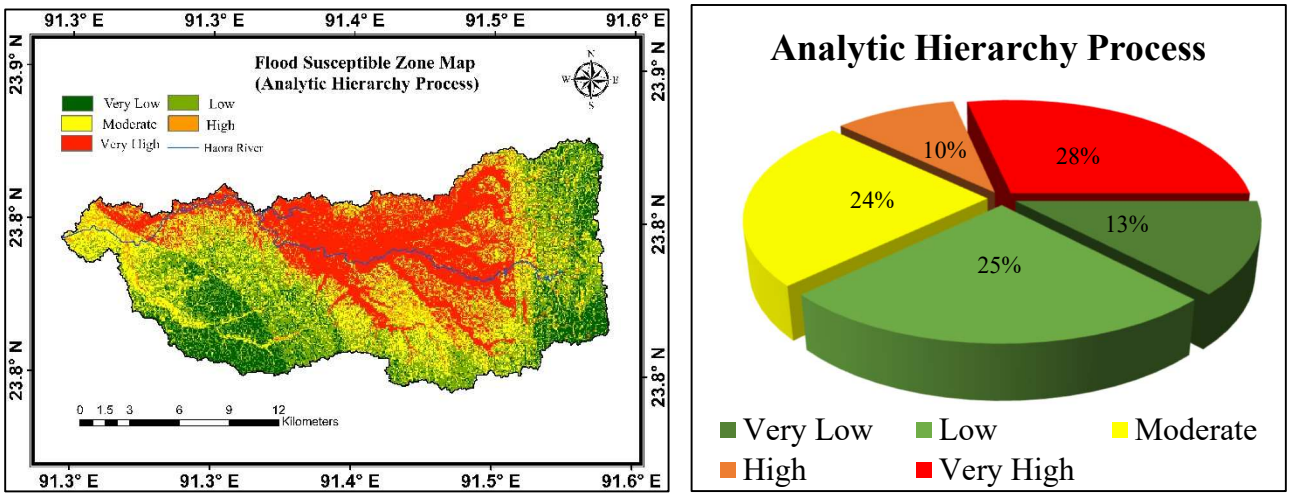

Figure 6: Classification of Flood-Susceptibility Zonation According to the AHP Method (Left) and Percentage-wise Classification of Flood-Prone Areas in the Haora River Basin (Right)

The weights and rankings assigned to the parameters were calculated using the AHP method. *Table 4* outlines the classification, ranking, and weightage of the parameters used in this study, while *Table 5* provides the final weightage values derived from the AHP calculations. Rainfall emerged as the most influential parameter, receiving the highest weightage of 0.27, followed closely by elevation (0.26) and slope (0.21). These parameters were identified as critical determinants of flood susceptibility, given their significant role in influencing surface runoff and flood dynamics.

Conversely, geomorphology and profile curvature, each assigned a weightage of 0.02, were determined to have the least impact on flood susceptibility in the study area. The consistency index (CI) value of 0.095, which is below the acceptable threshold of 0.10, confirms the reliability and robustness of the weightage assignments and ensures the credibility of the AHP methodology adopted in this study.

Table 4: Flood Susceptibility Assessment Parameter with Classifications, Rankings, and Weightages

Parameters	Class	Ranking	Weightage
Rainfall (mm)	2288–2310	1	0.27
	2310–2331	2	
	2331–2353	3	
	2353–2374	4	
	2374–2396	5	
LULC	Water	5	0.03
	Forest	2	
	Crop Land	3	
	Urban	4	
	Barren/Rangeland	1	
Elevation (m)	6-56	5	0.26
	56-107	4	
	107-157	3	
	157-208	2	
	208-258	1	
Proximity to the River (km)	<2	5	0.07
	2-3	4	
	3-4	3	
	4-6	2	
	6-8	1	
Slope (Degree)	<7.8	5	0.21
	7.8-15.6	4	
	15.6-23.4	3	
	23.4-31.2	2	
	31.2-39	1	
Flow Accumulation (pixels)	1–44111	1	0.06
	44112-88222	2	
	88223-132333	3	
	132334-176444	4	
	176445-220553	5	
Geomorphology	Flat Areas	5	0.02
	Gently Sloping Areas	4	
	Moderately Sloped	3	
	Moderate Relief	2	
	Steep Areas	1	
Topography Wetness Index	3-7	1	0.06
	7-11	2	
	11-15	3	
	15-19	4	
	19-22	5	
Profile Curvature	-3 to -1.8	1	0.02
	-1.8 to -0.6	2	
	-0.6 to 0.6	3	
	0.6 to 1.8	4	
	1.8 to 3	5	

The calculated weights were applied to derive the FSI, which was then spatially mapped to illustrate the distribution of flood susceptibility across the study area. The study revealed that the

area under the "Very Low" flood-prone category spans 12.89 km², while the "Low" category covers 24.97 km². Similarly, the "Moderate" flood-prone zone accounts for 24.14 km², followed by the "High" category with 9.65 km². The "Very High" flood-prone zone emerged as the largest, occupying 28.36 km² of the total study area. This spatial distribution highlights significant variations in flood susceptibility, with specific areas being more vulnerable to flooding than others.

Table 5: Pairwise Comparison Matrix for Flood-Prone Area Assessment Using the AHP Method

	Rainfall	Elevation	Slope	Proximity to the River	Flow Accumulation	TWI	LULC	Geomorphology	Profile Curvature
Rainfall	1	2	2	5	4	6	8	6	9
Elevation	0.5	1	3	6	4	7	6	8	9
Slope	0.5	0.33	1	5	8	7	5	6	6
Proximity to the River	0.2	0.17	0.2	1	2	2	4	5	3
Flow Accumulation	0.25	0.25	0.12	0.5	1	2	3	5	4
TWI	0.17	0.14	0.14	0.5	0.5	1	4	6	5
LULC	0.12	0.17	0.2	0.25	0.33	0.25	1	2	3
Geomorphology	0.17	0.12	0.17	0.2	0.2	0.17	0.5	1	2
Profile Curvature	0.111	0.11	0.17	0.33	0.25	0.2	0.33	0.5	1

The dominance of the "Very High" flood-prone zone underscores the vital need for targeted flood management policies in these regions. These findings emphasize the critical role of rainfall, elevation, and slope in determining flood vulnerability, while parameters such as geomorphology and profile curvature play a comparatively minor role. The resulting FSZ map delivers valuable understandings into flood dynamics within the Haora River Basin, offering a robust tool for flood management, preparedness, and mitigation planning. This study not only enhances the understanding of flood-prone areas but also serves as a decision-support framework for stakeholders aiming to reduce flood risks and their associated impacts in the region.

To classify the Flood Susceptibility Index (FSI), multiple classification schemes—including natural breaks (Jenks), quantile, and equal interval—were evaluated. While natural breaks often

optimize class boundaries by minimizing intra-class variance, and quantile ensures equal area distribution across classes, we selected the equal interval method to maintain consistent class ranges and preserve the continuous structure of the FSI values. This approach provided a more balanced visual interpretation and facilitated easier comparison between zones, particularly for policy and planning purposes. Nonetheless, future studies may explore dynamic classification methods depending on data skewness and application needs.

4.3. Results of Machine Learning-Based Flood Susceptibility Mapping

Flood susceptibility maps were generated using both the RF and SVM models based on nine conditioning factors. The output maps were classified into five susceptibility zones: very low, low, moderate, high, and very high, enabling spatial interpretation of flood vulnerability across the Haora River Basin.

The RF-derived map in *Figure 7* reveals that the central and northern parts of the basin, particularly along the Haora River corridor, are predominantly classified under high to very high flood susceptibility, while the southern and eastern regions fall under low to moderate categories. According to the RF classification summary, approximately 28% of the area falls under the high category and 15% under very high, indicating significant flood-prone zones.

The SVM-based flood map, *Figure 7*, presents a similar spatial pattern but with slight differences in distribution intensity. In this case, 29% of the basin area was classified as moderately susceptible, while 19% fell under very high and another 19% under high susceptibility. The overall pattern is consistent with observed flood-prone areas, confirming model reliability.

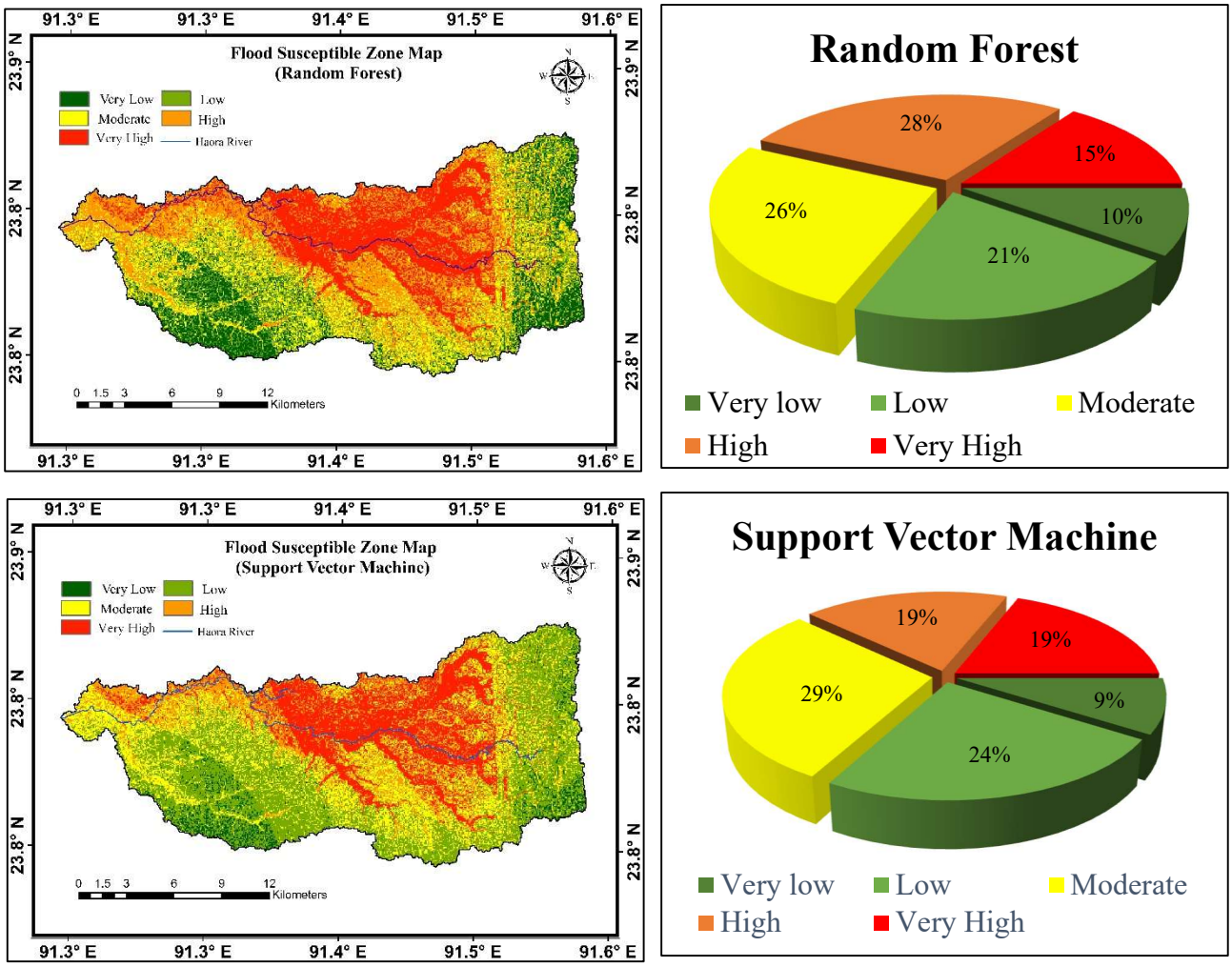

Figure 7: Classification of Flood-Susceptibility Zonation According to the SVM (Left) and Percentage-wise Classification of Flood-Prone Areas in the Haora River Basin (Right)

The statistical performance of the machine learning models was assessed using three standard error metrics: MAE, MSE, and RMSE for both the training and validation phases (see *Table 6*). The RF model demonstrated stronger predictive performance with a training MAE of 0.0195 and validation MAE of 0.0487, indicating minimal deviation between predicted and actual flood susceptibility values. The corresponding MSE values were 0.0142 (training) and 0.0228 (validation), while the RMSE values were recorded as 0.1192 and 0.4775, respectively.

Table 6: Statistical error metrics for RF and SVM models during training and validation phases, reflecting model accuracy in predicting flood susceptibility.

Models	MAE		MSE		RMSE	
	Training	Validation	Training	Validation	Training	Validation
RF	0.0195	0.0487	0.0142	0.0228	0.1192	0.4775
SVM	0.0884	0.1035	0.0262	0.0317	0.1619	0.1780

In comparison, the SVM model exhibited higher error margins, with MAE values of 0.0884 (training) and 0.1035 (validation), and MSE values of 0.0262 and 0.0317, respectively. The RMSE for SVM reached 0.1619 during training and 0.1780 during validation. These results collectively indicate that the RF model not only generalized better to unseen data but also maintained a lower prediction error across all metrics. Thus, Random Forest outperformed SVM in terms of statistical robustness and predictive reliability for flood susceptibility mapping in the Haora River Basin.

4.4. Stillwell Ranking Methods for Sensitivity Analysis

This study applied sensitivity analysis to assess the significance of each thematic layer and its impact on the delineation of flood-prone zones within the Haora River Basin. The analysis focused on understanding the effect of assigned ranks and weights for each class and thematic layer in determining the final flood-prone index FSI values. This process also helped identify which thematic layers have the most or least influence in shaping the spatial distribution of flood-prone zones.

The Stillwell ranking method was applied to compare the weightage derived from the APH with alternative methods, such as RSW and RRW. *Figure 8* compares the weightages between AHP, RSW, and RRW. At the same time, *Table 7* illustrates the comparative weightages, revealing no significant variations in the criteria ranking across these methods, demonstrating consistency in the prioritization of influential parameters.

Table 7: Comparison of AHP Weight Assignments Using Various Methods for Flood-Prone Area Zonation

Parameters	**Saaty (1980)**		**Ranking methods: Stillwell (1981)**			
	Pair wise		Rank Sum (RS)		Rank Reciprocal (RR)	
	AHP	Direct Rank	$(n - r_j + 1)$	$\frac{(n - r\_j + 1)}{\sum(n - r_j + 1)}$	$1/r_j$	$\frac{1/r_j}{\sum 1/r_j}$
Rainfall	0.268	1	9	0.200	1.000	0.353
Elevation	0.261	2	8	0.178	0.500	0.177
Slope	0.208	3	7	0.156	0.333	0.118
Proximity to the River	0.073	4	6	0.133	0.250	0.088
Flow Accumulation	0.064	5	5	0.111	0.200	0.071
TWI	0.057	6	4	0.089	0.167	0.059
LULC	0.030	7	3	0.067	0.143	0.050
Geomorphology	0.022	8	2	0.044	0.125	0.044
Profile Curvature	0.018	9	1	0.022	0.111	0.039

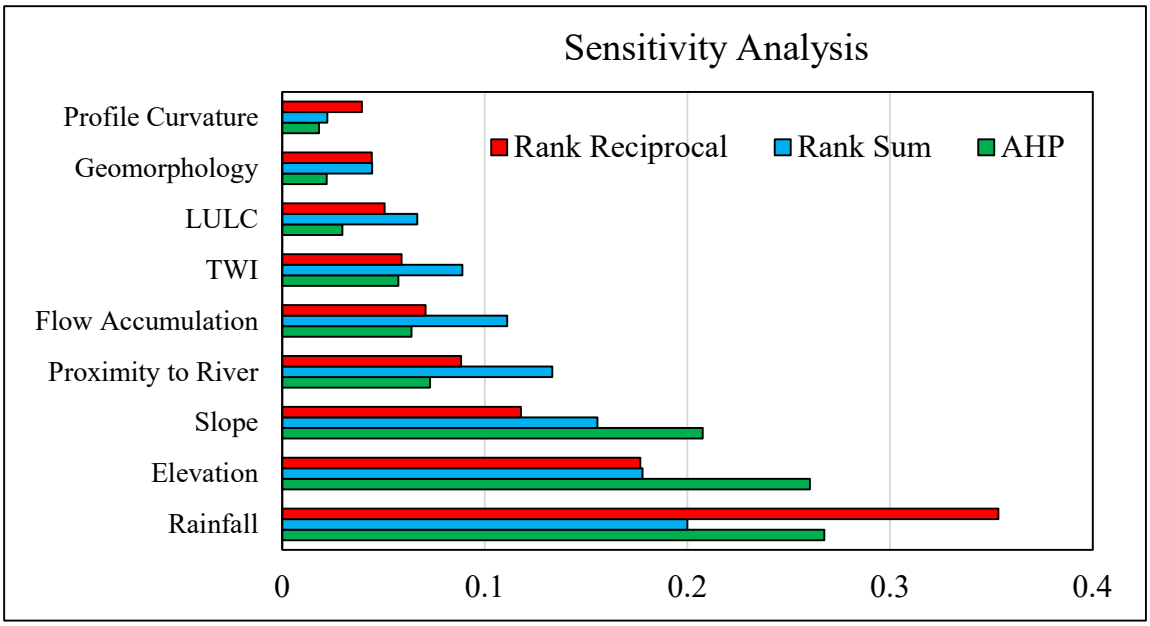

Figure 8: Bar Plot Comparing the Weightage for Flood-Prone Zonation Using Different Methods: AHP vs. Rank Reciprocal and Rank Sum.

This analysis validates the robustness of the AHP-derived weights while emphasizing the importance of rainfall, elevation, and slope as key contributors to flood susceptibility in the Haora River Basin. Conversely, parameters like geomorphology and profile curvature, which were

assigned lower weights, also demonstrated consistent rankings, confirming their limited influence. Overall, the Stillwell ranking methods provide an additional layer of confidence in the AHP-based flood-prone zone mapping approach for the Haora River Basin.

4.5. Validation of Flood-Prone Zone Mapping Using ROC-AUC Assessments

The predictive accuracy of the AHP, RF, and SVM models was evaluated using the AUC metric derived from the ROC analysis. The results, illustrated in *Figure 9,* reveal varying levels of model performance. The AHP model achieved an AUC value of 0.8485, placing it in the "acceptable" category (0.8–0.9), which indicates good classification ability in delineating flood-prone areas across the Haora River Basin. For the machine learning models, both RF and SVM demonstrated higher predictive accuracy. The RF model recorded AUC scores of 0.8932 and 0.9483 under different training scenarios, reflecting excellent performance (AUC > 0.9) in distinguishing flooded and non-flooded zones. The SVM model yielded AUC values of 0.8462 and 0.9260, indicating a performance ranging from "acceptable" to "excellent." These results confirm that while AHP offers a reliable baseline, the machine learning models—particularly Random Forest—provided superior classification capabilities for flood susceptibility mapping in the study area.

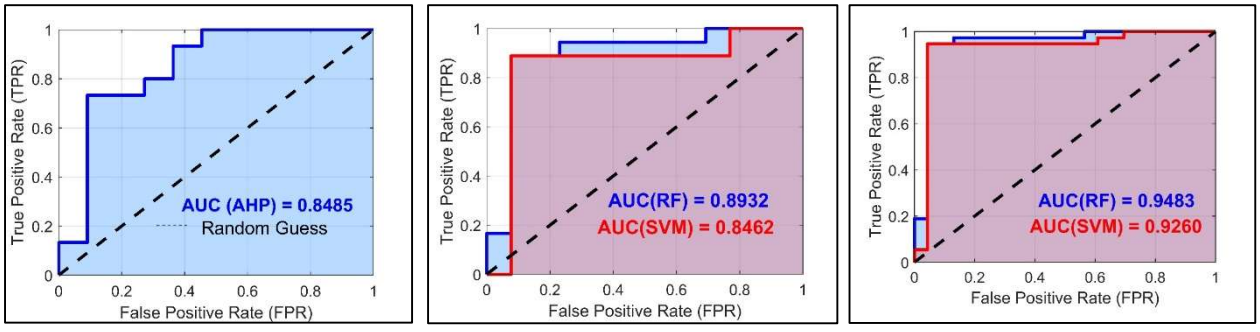

Figure 9: ROC curves showing the classification performance of AHP, RF, and SVM models for flood susceptibility mapping in the Haora River Basin.

4.6.Discussion

The flood susceptibility assessment of the Haora River Basin reveals significant hydrological vulnerability, particularly in the densely populated and low-lying areas surrounding Agartala. The integration of both AHP-GIS and machine learning approaches (RF, SVM) enabled a robust analysis that highlights rainfall, elevation, and slope as dominant flood-conditioning parameters. Rainfall, with a weightage of 0.27, reflects the region's monsoonal intensity, which frequently triggers rapid runoff and urban inundation. The high sensitivity to elevation (0.26) and slope (0.21) also underscores the role of terrain in modulating flood pathways, especially in urbanized floodplains.

The spatial distribution of flood-susceptible zones shows a concentration of "High" and "Very High" susceptibility in central and northern parts of the basin, particularly along the Haora River corridor. These patterns are consistent with earlier findings by (Ahmed et al., 2024; Chakraborty & Pan, 2012), which also identified the Haora and nearby river systems as among the most flood-sensitive in Northeast India. However, unlike previous studies, the present work combines expert-driven (AHP) and data-driven (RF, SVM) techniques within a common geospatial platform. This integration enhances predictive reliability and compensates for the limitations of using either approach in isolation.

The novelty of this study lies not only in the application of the traditional AHP-GIS approach but in its methodological synthesis that combines expert-driven techniques with machine learning-based models to enhance predictive performance. The parameter refinement and modeling framework was specifically tailored to the data-scarce and topographically complex terrain of Tripura. The integration of Random Forest and Support Vector Machine models alongside AHP not only strengthened model robustness but also demonstrated the value of hybrid approaches in

flood risk assessment for small, data-constrained basins. This is consistent with previous research, such as Gholami et al. 2025 and Mohammadifar et al. 2023 which showed that integrating machine learning models with traditional decision-making techniques improves flood prediction accuracy, especially in data-limited environments.

The RF model, in particular, showed superior performance with an AUC of 0.9483 and the lowest validation error metrics, establishing it as a robust tool for future flood susceptibility mapping in similar physiographic settings. The SVM model also performed well but exhibited slightly higher error rates, reaffirming that ensemble methods like RF offer better generalization in complex, non-linear flood systems. Demissie et al., 2024, similarly found Random Forest to outperform both SVM and logistic regression in flood susceptibility modeling, attributing this to RF's robustness in handling high-dimensional, non-linear datasets.

Among the three models, Random Forest emerged as the most accurate and reliable approach, offering the lowest error margins and highest classification performance. The Support Vector Machine, while performing better than AHP in terms of predictive accuracy, was slightly less consistent than RF. The AHP-GIS method, despite its subjectivity, provided a good baseline assessment and spatial interpretability, especially valuable in data-scarce contexts.

This research not only confirms the utility of AHP-GIS frameworks for flood risk assessment but also demonstrates the added value of integrating machine learning models to improve objectivity, accuracy, and spatial resolution. The proposed methodology is generalizable and adaptable to other urban catchments across Tripura and similar data-constrained basins in Northeast India and beyond. In conclusion, this study provides a technically sound, scalable, and policy-relevant framework for flood susceptibility assessment, contributing significantly to resilient urban planning, disaster preparedness, and climate adaptation strategies in the region.

The study also holds direct policy relevance for flood risk governance in Agartala, the capital of Tripura. The FSZ map serves as a decision-support tool to guide municipal planners and disaster management agencies in identifying priority areas for structural and non-structural mitigation. Zones under "Very High" susceptibility demand targeted interventions such as levee construction, improved urban drainage systems, enforcement of no-development zones, and restoration of natural floodplains. Integrating this spatial output into the city's master planning, zoning regulations, and early warning protocols can significantly reduce flood exposure. Furthermore, these high-risk areas offer opportunities for implementing nature-based solutions such as urban green buffers, rainwater harvesting zones, and retention ponds to enhance flood resilience. The FSZ map can also support evidence-based resource allocation, improve emergency preparedness, and inform future land use decisions in a rapidly urbanizing floodplain.

Nonetheless, the study has several limitations. The absence of real-time hydrological inputs, such as water level and discharge measurements, constrained the temporal dynamics of flood prediction. The reliance on subjective expert judgment in AHP, although mitigated through sensitivity analysis and model comparison, still introduces a degree of bias. The exclusion of socio-economic vulnerability indicators, such as population density, housing quality, and critical infrastructure which limits the risk analysis to physical exposure alone.

Future research could address these gaps by integrating real-time flood forecasting systems, which are already being piloted in cities like Pune (India) and Jakarta (Indonesia) through IoT-based sensors and satellite-radar integration. Moreover, the use of Fuzzy AHP, entropy weighting, or hybrid MCDM–ML frameworks could reduce subjectivity and enhance modeling robustness. The inclusion of social vulnerability datasets from census and municipal sources would enable a shift from flood susceptibility mapping to comprehensive flood risk assessment.

Overall, this study advances flood-prone mapping methodologies by demonstrating that a synergistic approach—combining expert knowledge and machine learning—can effectively delineate flood vulnerability in small, data-constrained river basins. It offers both scientific rigor and policy-oriented outputs that are essential for flood-resilient urban planning in the Haora River Basin and beyond.

5. Concluding Remarks

This study successfully delineated flood-susceptible zones (FSZ) in the Haora River Basin, a hydrologically vulnerable region within the West Tripura district, by integrating the Analytic Hierarchy Process (AHP) with Geographic Information System (GIS) tools. Additionally, to improve model accuracy and reduce subjectivity, machine learning models like Random Forest (RF) and Support Vector Machine (SVM) were also applied, offering a comparative and hybrid framework for flood susceptibility assessment in data-scarce basins. A total of nine flood-conditioning parameters were considered, including topographic, hydrological, and land-use variables. The study produced multiple susceptibility maps that collectively provide a detailed understanding of flood-prone areas in the basin. The major findings are summarized below:

I. Rainfall was identified as the most influential parameter in flood susceptibility, receiving a weightage of 0.27, followed by elevation (0.26) and slope (0.21), highlighting the role of intense monsoonal precipitation and terrain characteristics in influencing flood behavior.
II. The AHP-derived FSZ map showed that the "Very High" flood-prone zone accounts for the largest area (28%), confirming substantial hydrological vulnerability, especially in low-lying, urbanized regions near Agartala.
III. In comparison, the RF model identified 15% and the SVM model delineated 19% of the total catchment area under the "Very High" susceptibility category. Although there are

minor differences in spatial extent, all three models consistently highlighted the central basin and Agartala region as zones of elevated flood risk.

IV. The AHP model achieved an ROC-AUC value of 0.8485, indicating "acceptable" predictive accuracy. In comparison, the RF model attained an AUC of 0.9483, and SVM recorded 0.9260, both falling into the "excellent" category, demonstrating the superior predictive capability of machine learning approaches.

V. Among the three approaches, Random Forest emerged as the most accurate and reliable model for flood susceptibility mapping. At the same time, AHP offered valuable expert-driven spatial interpretation, and SVM provided a strong intermediate performance.

This research confirms the utility of the AHP-GIS framework and demonstrates the added value of integrating machine learning to enhance model accuracy and objectivity. While the methodology is generalizable to other flood-prone, data-scarce basins, the current study is limited by the absence of dynamic hydrological data and socio-economic indicators. Future work may address these gaps by incorporating real-time monitoring systems and broader vulnerability metrics. Overall, the FSZ map developed in this study can serve as a planning tool for Agartala's municipal authorities by identifying high-risk flood zones where interventions such as improved drainage, land-use zoning restrictions, and early warning systems should be prioritized to enhance urban flood resilience.

References

Abdelkareem, M., & Mansour, A. M. (2023). Risk assessment and management of vulnerable areas to flash flood hazards in arid regions using remote sensing and GIS-based knowledge-driven techniques. *Natural Hazards*, *117*(3), 2269–2295. https://doi.org/10.1007/s11069-023-05942-x

Agrawal, R., Singh, S. K., Kanga, S., Sajan, B., Meraj, G., & Kumar, P. (2024). Advancing Flood Risk Assessment through Integrated Hazard Mapping: A Google Earth Engine-Based Approach for Comprehensive Scientific Analysis and Decision Support. *Journal of Climate Change*, *10*(1), 47–60. https://doi.org/10.3233/jcc240007

Ahmed, I., Das (Pan), N., Debnath, J., Bhowmik, M., & Bhattacharjee, S. (2024). Flood hazard zonation using GIS-based multi-parametric Analytical Hierarchy Process. *Geosystems and Geoenvironment*, *3*(2). https://doi.org/10.1016/j.geogeo.2023.100250

Alabbad, Y., Mount, J., Campbell, A. M., & Demir, I. (2021). Assessment of transportation system disruption and accessibility to critical amenities during flooding: Iowa case study. *Science of the Total Environment*, *793*, 148476. https://doi.org/10.1016/j.scitotenv.2021.148476

Alam, Z., Ali, Y., & Pamucar, D. (2024). Elevating Pakistan's flood preparedness: a fuzzy multi-criteria decision making approach. *Financial Innovation*, *10*(1). https://doi.org/10.1186/s40854-024-00659-7

Al-Omari, A. A., Shatnawi, N. N., Shbeeb, N. I., Istrati, D., Lagaros, N. D., & Abdalla, K. M. (2024). Utilizing Remote Sensing and GIS Techniques for Flood Hazard Mapping and Risk Assessment. *Civil Engineering Journal (Iran)*, *10*(5), 1423–1436. https://doi.org/10.28991/CEJ-2024-010-05-05

Bales, J. D., & Wagner, C. R. (2009). Sources of uncertainty in flood inundation maps. Journal of Flood Risk Management, 2(2), 139–147. https://doi.org/10.1111/j.1753-318X.2009.01029.x

Bandyopadhyay, S., Ghosh, K., & De, S. K. (2014). A proposed method of bank erosion vulnerability zonation and its application on the River Haora, Tripura, India. *Geomorphology*, *224*, 111–121. https://doi.org/10.1016/j.geomorph.2014.07.018

Chakraborty, M., & Pan, N. Das. (2012). Effect Of Flood On Land Use In Different Return Periods : A Case Study From The Lower Haora. *Indian Streams Research Journal*, *2*(7), 1–7.

Chaudhary, M. T., & Piracha, A. (2021). *Natural Disasters — Origins , Impacts , Management*. 1101–1131.

Darabi, H., Haghighi, A. T., Mohamadi, M. A., Rashidpour, M., Ziegler, A. D., Hekmatzadeh, A. A., & Kløve, B. (2020). Urban flood risk mapping using data-driven geospatial techniques for a flood-prone case area in Iran. *Hydrology Research*, *51*(1), 127–142. https://doi.org/10.2166/nh.2019.090

Debnath, J., Das, N., & Sahariah, D. (2022). Impacts of temperature–rainfall and land use/land cover changes on the hydrological regime in the Muhuri River basin, Northeast India. *Sustainable Water Resources Management*, *8*(5), 1–21. https://doi.org/10.1007/s40899-022-

00738-6

Demissie, Z., Rimal, P., Seyoum, W. M., Dutta, A., & Rimmington, G. (2024). Flood susceptibility mapping: Integrating machine learning and GIS for enhanced risk assessment. *Applied Computing and Geosciences*, *23*(March), 100183. https://doi.org/10.1016/j.acags.2024.100183

Deo, P., Siddiqui, M. A., Siddiqui, L., Naqvi, H. R., Faruque, U., & Dwivedi, D. (2024). An integrated approach for urban flood risk prediction using AHP-TOPSIS model: a case study of Jaipur region. In *Natural Hazards* (Issue 0123456789). Springer Netherlands. https://doi.org/10.1007/s11069-024-06965-8

Efraimidou, E., & Spiliotis, M. (2024). A GIS-Based Flood Risk Assessment Using the Decision-Making Trial and Evaluation Laboratory Approach at a Regional Scale. In *Environmental Processes* (Vol. 11, Issue 1). Springer International Publishing. https://doi.org/10.1007/s40710-024-00683-w

Fang, L., Huang, J., Cai, J., & Nitivattananon, V. (2022). Hybrid approach for flood susceptibility assessment in a flood-prone mountainous catchment in China. *Journal of Hydrology*, *612*(PA), 128091. https://doi.org/10.1016/j.jhydrol.2022.128091

Feng, D., Shi, X., & Renaud, F. G. (2023). Risk assessment for hurricane-induced pluvial flooding in urban areas using a GIS-based multi-criteria approach: A case study of Hurricane Harvey in Houston, USA. *Science of the Total Environment*, *904*(September), 166891. https://doi.org/10.1016/j.scitotenv.2023.166891

Gholami, H., Mohammadifar, A., Golzari, S., Torkamandi, R., Moayedi, E., Zare Reshkooeiyeh, M., Song, Y., & Zeeden, C. (2025). Mapping flood risk using a workflow including deep learning and MCDM– Application to southern Iran. Urban Climate, 59(September 2024), 102272. https://doi.org/10.1016/j.uclim.2024.102272

Ghosh, S., Saha, S., & Bera, B. (2022). Flood susceptibility zonation using advanced ensemble machine learning models within Himalayan foreland basin. *Natural Hazards Research*, *2*(4), 363–374. https://doi.org/10.1016/j.nhres.2022.06.003

Hadian, S., Afzalimehr, H., Soltani, N., Shahiri Tabarestani, E., & Pham, Q. B. (2022). Application of MCDM methods for flood susceptibility assessment and evaluation the impacts of past experiences on flood preparedness. *Geocarto International*, *37*(27), 16283–16306. https://doi.org/10.1080/10106049.2022.2107714

Hamizahrul, F. Y. (2024). *Optimizing Supplier Selection : Leveraging Analytic Hierarchy Process (AHP) in Purchasing Decision Support Systems*. *18*(1), 11–21.

Hoang, D. V., & Liou, Y. A. (2024). Assessing the influence of human activities on flash flood susceptibility in mountainous regions of Vietnam. *Ecological Indicators*, *158*(December 2023), 111417. https://doi.org/10.1016/j.ecolind.2023.111417

Hossain, B., Sarker, M. N. I., & Sohel, M. S. (2024). Flooded lives: socio-economic implications and adaptation challenges for riverine communities in Bangladesh. *International Journal of Environmental Science and Technology*, *0123456789*. https://doi.org/10.1007/s13762-024-05943-8

Idrees, M. O., Olateju, S. A., Omar, D. M., Babalola, A., Ahmadu, H. A., & Kalantar, B. (2022). Spatial assessment of accelerated surface runoff and water accumulation potential areas using AHP and data-driven GIS-based approach: the case of Ilorin metropolis, Nigeria. *Geocarto International*, *37*(27), 15877–15895. https://doi.org/10.1080/10106049.2022.2102236

Jain, S. K., & Singh, V. P. (2023). Strategies for flood risk reduction in India. *ISH Journal of Hydraulic Engineering*, *29*(2), 165–174. https://doi.org/10.1080/09715010.2021.2019136

Janizadeh, S., Chandra Pal, S., Saha, A., Chowdhuri, I., Ahmadi, K., Mirzaei, S., Mosavi, A. H., & Tiefenbacher, J. P. (2021). Mapping the spatial and temporal variability of flood hazard affected by climate and land-use changes in the future. *Journal of Environmental Management*, *298*(July), 113551. https://doi.org/10.1016/j.jenvman.2021.113551

Jha, M. K., & Afreen, S. (2020). Flooding urban landscapes: Analysis using combined hydrodynamic and hydrologic modeling approaches. *Water (Switzerland)*, *12*(7). https://doi.org/10.3390/w12071986

Kara, R., & Singh, P. (2024). Flood assessment for Lower Godavari basin by using the application of GIS-based analytical hierarchy process. *International Journal of System Assurance Engineering and Management*, *0123456789*. https://doi.org/10.1007/s13198-024-02595-2

Kassegn, A., & Endris, E. (2021). Review on socio-economic impacts of 'Triple Threats' of COVID-19, desert locusts, and floods in East Africa: Evidence from Ethiopia. *Cogent Social Sciences*, *7*(1). https://doi.org/10.1080/23311886.2021.1885122

Kaya, C. M., & Derin, L. (2023). Parameters and methods used in flood susceptibility mapping: a review. *Journal of Water and Climate Change*, *14*(6), 1935–1960. https://doi.org/10.2166/wcc.2023.035

Kiani, A., Motamedvaziri, B., khaleghi, M. R., & Ahmadi, H. (2024). Investigating the flood potential of basins to locate the implementation of remedial operations in the Siah Khor watershed using VIKOR, TOPSIS, and HEC-HMS model (case study: Siah Khor watershed-Islamabad west). *Environmental Earth Sciences*, *83*(18). https://doi.org/10.1007/s12665-024-11847-0

Kumar, M., Sharif, M., & Ahmed, S. (2020). Impact of urbanization on the river Yamuna basin. *International Journal of River Basin Management*, *18*(4), 461–475. https://doi.org/10.1080/15715124.2019.1613412

Kumar, R. (2025). *A Comprehensive Review of MCDM Methods , Applications , and Emerging Trends*. *3*(1), 185–199.

Kumar, R., Kumar, M., Tiwari, A., Majid, S. I., Bhadwal, S., Sahu, N., & Avtar, R. (2023). Assessment and Mapping of Riverine Flood Susceptibility (RFS) in India through Coupled Multicriteria Decision Making Models and Geospatial Techniques. *Water (Switzerland)*, *15*(22). https://doi.org/10.3390/w15223918

Kumar, S. B. S. (2017). *Interference on River Health*.

Kuntal, G. (2015). Spatio-Temporal Analysis of Flood and Identification of Flood Hazard Zone of

West Tripura District , Tripura , Spatio-Temporal Analysis of Flood and Identification of Flood Hazard Zone of West Tripura District , Tripura ,. *Hill Geographer*, *January*.

Le Cozannet, G., Garcin, M., Bulteau, T., Mirgon, C., Yates, M. L., Méndez, M., Baills, A., Idier, D., & Oliveros, C. (2013). An AHP-derived method for mapping the physical vulnerability of coastal areas at regional scales. *Natural Hazards and Earth System Science*, *13*(5), 1209–1227. https://doi.org/10.5194/nhess-13-1209-2013

Leta, B. M., & Adugna, D. (2023). Identification and mapping of flood-prone areas using GIS-based multi-criteria decision-making and analytical hierarchy process: the case of Adama City's watershed, Ethiopia. *Applied Geomatics*, *15*(4), 933–955. https://doi.org/10.1007/s12518-023-00532-9

Liu, Q., Yuan, J., Yan, W., Liang, W., Liu, M., & Liu, J. (2023). Association of natural flood disasters with infectious diseases in 168 countries and territories from 1990 to 2019: A worldwide observational study. *Global Transitions*, *5*(38), 149–159. https://doi.org/10.1016/j.glt.2023.09.001

Mabrouk, M., & Haoying, H. (2023). Urban resilience assessment: A multicriteria approach for identifying urban flood-exposed risky districts using multiple-criteria decision-making tools (MCDM). *International Journal of Disaster Risk Reduction*, *91*(April), 103684. https://doi.org/10.1016/j.ijdrr.2023.103684

Manzoor, Z., Ehsan, M., Khan, M. B., Manzoor, A., Akhter, M. M., Sohail, M. T., Hussain, A., Shafi, A., Abu-Alam, T., & Abioui, M. (2022). Floods and flood management and its socio-economic impact on Pakistan: A review of the empirical literature. *Frontiers in Environmental Science*, *10*(December), 1–14. https://doi.org/10.3389/fenvs.2022.1021862

Marquaridt, D. W. (1970). Generalized inverses, ridge regression, biased linear estimation, and nonlinear estimation. *Technometrics*, *12*(3), 591–612. https://doi.org/10.1080/00401706.1970.10488699

Mitra, R., Saha, P., & Das, J. (2022). Assessment of the performance of GIS-based analytical hierarchical process (AHP) approach for flood modelling in Uttar Dinajpur district of West Bengal, India. *Geomatics, Natural Hazards and Risk*, *13*(1), 2183–2226. https://doi.org/10.1080/19475705.2022.2112094

Mohammadifar, A., Gholami, H., & Golzari, S. (2023). Novel integrated modelling based on multiplicative long short-term memory (mLSTM) deep learning model and ensemble multi-criteria decision making (MCDM) models for mapping flood risk. *Journal of Environmental Management*, *345*(June), 118838. https://doi.org/10.1016/j.jenvman.2023.118838

Mukherjee, I., & Singh, U. K. (2020). Delineation of groundwater potential zones in a drought-prone semi-arid region of east India using GIS and analytical hierarchical process techniques. Catena, 194(December 2019), 104681. https://doi.org/10.1016/j.catena.2020.104681

Munawar, H. S., Hammad, A. W. A., & Waller, S. T. (2021). A review on flood management technologies related to image processing and machine learning. *Automation in Construction*, *132*(September), 103916. https://doi.org/10.1016/j.autcon.2021.103916

Munpa, P., Dubsok, A., Phetrak, A., Sirichokchatchawan, W., Taneepanichskul, N., Lohwacharin, J., Kittipongvises, S., & Polprasert, C. (2024). Building a Resilient City through Sustainable Flood Risk Management: The Flood-Prone Area of Phra Nakhon Sri Ayutthaya, Thailand. *Sustainability (Switzerland)*, *16*(15). https://doi.org/10.3390/su16156450

Nath, N. K., Gautam, V. K., Pande, C. B., Mishra, L. R., Raju, J. T., Moharir, K. N., & Rane, N. L. (2024). Development of landslide susceptibility maps of Tripura, India using GIS and analytical hierarchy process (AHP). *Environmental Science and Pollution Research*, *31*(5), 7481–7497. https://doi.org/10.1007/s11356-023-31486-5

Paul, A.R., Saha, A. K. (2021). (2021). Indicator Based Impact Analysis of Urbanization with Respect to Evapo-Transpiration. In: Majumder, M., Kale, G.D. (eds) Water and Energy Management in India. Springer, Cham. https://doi.org/10.1007/978-3-030-66683-5_3. In *Water and Energy Management in India*. https://doi.org/10.1007/978-3-030-66683-5

Pizzorni, M., Innocenti, A., & Tollin, N. (2024). Droughts and floods in a changing climate and implications for multi-hazard urban planning: A review. *City and Environment Interactions*, *24*(September), 100169. https://doi.org/10.1016/j.cacint.2024.100169

Prokešová, R., Horáčková, Š., & Snopková, Z. (2022). Surface runoff response to long-term land use changes: Spatial rearrangement of runoff-generating areas reveals a shift in flash flood drivers. *Science of the Total Environment*, *815*. https://doi.org/10.1016/j.scitotenv.2021.151591

Rahman, H. U., Raza, M., Afsar, P., Alharbi, A., Ahmad, S., & Alyami, H. (2021). Multi-criteria decision making model for application maintenance offshoring using analytic hierarchy process. *Applied Sciences (Switzerland)*, *11*(18). https://doi.org/10.3390/app11188550

Rahman, M. M., Shobuj, I. A., Islam, M. R., Islam, M. R., Hossain, M. T., Alam, E., Hattawi, K. S. Al, & Islam, M. K. (2024). Flood preparedness in rural flood-prone area: a holistic assessment approach in Bangladesh. *Geomatics, Natural Hazards and Risk*, *15*(1). https://doi.org/10.1080/19475705.2024.2379599

Ramkar, P., & Yadav, S. M. (2021). Flood risk index in data-scarce river basins using the AHP and GIS approach. *Natural Hazards*, *109*(1), 1119–1140. https://doi.org/10.1007/s11069-021-04871-x

Rana, I. A., Asim, M., Aslam, A. B., & Jamshed, A. (2021). Disaster management cycle and its application for flood risk reduction in urban areas of Pakistan. *Urban Climate*, *38*(February), 100893. https://doi.org/10.1016/j.uclim.2021.100893

Rane, N. L., Achari, A., & Choudhary, S. P. (2023). Multi-Criteria Decision-Making (Mcdm) As a Powerful Tool for Sustainable Development: Effective Applications of Ahp, Fahp, Topsis, Electre, and Vikor in Sustainability. *International Research Journal of Modernization in Engineering Technology and Science*, *04*, 2654–2670. https://doi.org/10.56726/irjmets36215

Saaty, T. L. (1990). An Exposition of the AHP in Reply to the Paper "Remarks on the Analytic Hierarchy Process." *Management Science*, *36*(3), 259–268. https://doi.org/10.1287/mnsc.36.3.259

Saaty, T. L. (2004). Decision making — the Analytic Hierarchy and Network Processes

(AHP/ANP). *Journal of Systems Science and Systems Engineering*, *13*(1), 1–35. https://doi.org/10.1007/s11518-006-0151-5

Saha, A., Pal, S. C., Chowdhuri, I., Roy, P., Chakrabortty, R., & Shit, M. (2023). Vulnerability assessment of drought in India: Insights from meteorological, hydrological, agricultural and socio-economic perspectives. *Gondwana Research*, *123*, 68–88. https://doi.org/10.1016/j.gr.2022.11.006

Saha, S., Habib, A. S., Rahman, M. A., & Saha, M. (2021). Assessment of Water Quality of a Transboundary River at Brahmanbaria. *Bangladesh Journal of Zoology*, *49*(1), 137–146. https://doi.org/10.3329/bjz.v49i1.53689

Samansiri, S., Fernando, T., & Ingirige, B. (2022). Advanced Technologies for Offering Situational Intelligence in Flood Warning and Response Systems: A Literature Review. *Water (Switzerland)*, *14*(13). https://doi.org/10.3390/w14132091

Swain, K. C., Singha, C., & Nayak, L. (2020). Flood susceptibility mapping through the GIS-AHP technique using the cloud. ISPRS International Journal of Geo-Information, 9(12). https://doi.org/10.3390/ijgi9120720

Swets, J. (1988). Measuring the Accuracy of Diagnostic Systems Author(s): John A. Swets Source: *Science*, *240*(4857), 1285–1293.

Tehrany, M. S., Pradhan, B., & Jebur, M. N. (2014). Flood susceptibility mapping using a novel ensemble weights-of-evidence and support vector machine models in GIS. Journal of Hydrology, 512, 332–343. https://doi.org/10.1016/j.jhydrol.2014.03.008

Vilasan, R. T., & Kapse, V. S. (2022). Evaluation of the prediction capability of AHP and F-AHP methods in flood susceptibility mapping of Ernakulam district (India). *Natural Hazards*, *112*(2), 1767–1793. https://doi.org/10.1007/s11069-022-05248-4

Yu, Q., Wang, Y., & Li, N. (2022). Extreme Flood Disasters: Comprehensive Impact and Assessment. *Water (Switzerland)*, *14*(8), 1–14. https://doi.org/10.3390/w14081211